İSTANBUL TECHNICAL UNIVERSITY ⋆ INSTITUTE OF SCIENCE AND TECHNOLOGY

OSCILLATIONS AND RESONANT CONVERSION OF THE SOLAR NEUTRINOS

M.Sc THESIS

Phy. Hilmiye BALKAN

Date of Submission: 16 Ocak 1995

Date of Approval: 31 Ocak 1995

Supervisor: Prof. Dr. Jan KALAYCI

Members: Prof. Dr. Mahmut HORTAÇSU
Prof. Dr. Hasan KARADAYI

JANUARY 1995

İSTANBUL TEKNİK ÜNİVERSİTESİ ★ FEN BİLİMLERİ ENSTİTÜSÜ

SOLAR NÖTRİNOLARIN OSİLASYONLARI VE REZONANS DÖNÜŞÜMÜ

YÜKSEK LİSANS TEZİ

Fiz. Hilmiye BALKAN

Tezin Enstitüye verildiği Tarih: 16 Ocak 1995

Tezin Savunulduğu Tarih: 31 Ocak 1995

Tez Danışmanı: Prof. Dr. Jan KALAYCI

Diğer Jüri Üyeleri: Prof. Dr. Mahmut HORTAÇSU
Prof. Dr. Hasan KARADAYI

OCAK 1995

Acknowledgements

I am deeply grateful to my supervisor, Prof. Jan Kalaycı. I would like to express my gratitude to Prof. A. Yu. Smirnov for many interesting discussions and reading my thesis.

CONTENTS

LIST OF FIGURE v

LIST OF TABLES vi

SUMMARY vii

ÖZET viii

CHAPTER 1 EXPERIMENTAL DATA AND SOLAR NEUTRINO PROBLEM 1

1.1 Solar Neutrino Spectrum 1

1.2 Experimental Data 3

1.3 Solar Neutrino Problem 5

CHAPTER 2 NEUTRINO OSCILLATON AND RESONANT CONVERSION 7

2.1 Neutrino Oscillation In Vacuum 8

2.1.1 Neutrino Eigenstates 8

2.1.2 Evolution Equation And Its Solution 9

2.2 Neutrino Oscillation In Matter 11

2.2.1 Evolution Equation 11

2.2.2 Resonance Condition 13

2.2.3 Oscillations In Matter With Constant Density 15

2.2.4 Oscillation In Matter With Varying eDensity 16

CHAPTER 3 BOUNDS ON THE NEUTRINO PARAMETERS 21

3.1 Bounds On Neutrino Fluxes From Experimental Data . 21

3.2 General Constraint On $\triangle m^2$ 24

3.3 Small Mixing Solution 25

3.4 Large Mixing Solution 28

CHAPTER 4 CONCLUSION 30

REFERENCES 33

CURRICULUM VITAE

LIST OF FIGURES

Figure No. . . . . Page

Figure 1.1 Solar neutrino spectrum. This shows the energy spectrum of neutrinos that is predicted by the standard solar model. 3

Figure 2.1 The dependence of $\sin^2 2\theta_m$ on effective density of matter ($sin^2 2\theta_V = 0.1$, $\triangle m^2 = 10^{-4}\ eV^2$, $E_{res} = 4.533$ MeV). 15

Figure 2.2 The survival probability after crossing the layer of medium with constant density ($sin^2 2\theta_V = 0.1$, $\triangle m^2 = 10^{-4}\ eV^2$, distance traveled $R = 10^7$ km). 16

Figure 2.3 The dependence of eigenvalues on density. 18

Figure 2.4 The average survival probability in varying density ($sin^2 2\theta_V = 0.04$, $\triangle m^2 = 10^{-4}\ eV^2$). 19

Figure 3.1 General constraint on $\triangle m^2$. 26

Figure 3.2 The allowed region for small mixing case (f_B=1). 29

Figure 3.3 The allowed region for large mixing case (f_B=1). 30

Figure 4.1 Allowed regions for large mixing case: $f_B = 1, 1.5$ and for small mixing solution: $f_B = 1, 1.5$ (PART I). 32

Figure 4.2 Allowed regions for large mixing case: $f_B = 2, 2.5$ and for small mixing solution: $f_B = 0.75, 0.5$ (PART II). 33

LIST OF TABLES

Table No. . . . . Page

Table 1.1 Calculated solar neutrino fluxes. 2

Table 1.2 The solar neutrino data used in the analysis. 5

Table 1.3 Neutrino contribution to the calculated event rates. 6

Table 3.1 The effective survival probabilities. 24

SUMMARY

The predicted neutrino fluxes from the Sun according to the Standard Solar Models do not agree with the fluxes detected at the Earth. This disagreement is called the **"solar neutrino problem"**. In this work, we will study a possible solution of this problem in terms of the resonance flavour conversion (MSW effect). According to the **MSW effect**, during the propagation one neutrino state transforms to another state. We will see how the MSW effect can describe the experimental data for a large range of parameters.

In the first chapter, we will present the experimental data corresponding to the Standard Solar Model predictions and then formulate the solar neutrino problem.

In the second chapter, we will describe the neutrino oscillation and resonance conversion.

The comparison of the solar neutrino spectrum with experimental data will be given in the last chapter: we will find the allowed region for the parameters of the theory: Δm^2, $\sin^2 2\theta_V$. Moreover, we will study how the allowed regions are changed when the original Boron neutrino flux is changed.

ÖZET

Solar Nötrino Problemi

Dünyada nötrinolar doğal radyoaktivite, nükleer reaksiyonlar ve yüksek enerjili hızlandırıcılar tarafından üretilir. Güneşte ise nükleer füzyon sırasında meydana gelen zayıf etkileşmelerle üretilir. Zayıf, elektromanyetik ve gravitasyonel kuvvetlerde yer alan fakat kuvvetli etkileşmelerde yer almayan bir kütleli leptonla birleşmiş üç çeşit nötrino bilinmektedir. Bilinen leptonlar elektronlar, muonlar ve taulardır. Demek oluyor ki ν_e, ν_μ ve ν_τ nötrinoları vardır.

Güneşte nükleer reaksiyonlar tarafından üretilen nötrinolar "**solar nötrinolar**" diye adlandırılır. Biz bu nötrinolar üzerinde çalışacağız.

Solar nötrinoları üreten önemli iki reaksiyon ailesi vardır. Bunlar **pp-zinciri** ve **CNO-dönüşümü** diye adlandırılmaktadır.

pp-zincirinde en önemli nötrino-üreten reaksiyonlar aşağıda açık bir şekilde verilen *pp*, *pep*, *hep*, ^7Be ve ^8B reaksiyonlarıdır.

$$
\begin{aligned}
p + p &\rightarrow {}^2H + e^+ + \nu_e \quad (q \leq 0.420 MeV) \\
p + e^- + p &\rightarrow {}^2H + \nu_e \quad (q = 1.442 \;\; MeV) \\
{}^3He + p &\rightarrow {}^4He + \nu_e \quad (q \leq 18.773 \;\; MeV) \\
{}^7Be + e^- &\rightarrow {}^7Li + \nu_e \quad (q = 0.862 \;\; MeV, \; \%89.7; \\
q = 0.384 \;\; MeV, \; \%10.3) & \\
{}^8B &\rightarrow {}^7Be^* + e^+ + \nu_e \quad (q \leq 15 \;\; MeV)
\end{aligned}
$$

(q nötrino enerjisidir.)
pp, *hep* ve ^8B kaynaklarının her birinden elde edilen nötrinolar sürekli bir spektruma sahiptirler. *pep* ve ^7Be nötrinoları ise iyi tanımlanmış enerjilere sahiptirler ve spektrumları bir çizgi halindedir. **pp reaksiyonu** solar parlaklığın

yaklaşık olarak tamamını sağlayan zinciri başlattığından dolayı bu reaksiyondan elde edilen nötrinolar bir akıma en temeldir. pp nötrinoları düşük enerjilere sahiplerdir ve bu yüzden onları gözlemek zordur. Gözlenmesi en kolay nötrinolar *hep* ve ^8B reaksiyonlarından üretilen epeyce yüksek enerjili nötrinolardır.

CNO-dönüşümündeki temel reaksiyonlar ise aşağıda sırasıyla verilen ^{13}N, ^{15}O, ^{17}F reaksiyonlarıdır.

$$\begin{aligned} ^{13}N &\rightarrow {}^{13}C + e^+ + \nu_e \quad (q \leq 1.99 \;\; MeV) \\ ^{15}O &\rightarrow {}^{15}N + e^+ + \nu_e \quad (q \leq 1.732 \;\; MeV) \\ ^{17}F &\rightarrow {}^{17}O + e^+ + \nu_e \quad (q \leq 1.740 \;\; MeV) \end{aligned}$$

Fakat CNO nötrino kaynaklarının ne hesaplanmış akıların ne de karakteristik enerjilerin büyük olmamasından dolayı gözlenmelerinin zor olması beklenilir.

Solar nötrinolardaki mevcut data dört deneyden elde edilir. Bu deneyler **Homestake, Kamiokande, SAGE, GALLEX** olmaktadır. Bu deneylere göre elde edilen oranlar ile Standard Model'e göre tahmin edilen oran gözlenen orandan daha büyük ya da çok daha büyüktür. Kısaca, tahmin edilen nötrino akıları ile ölçülen nötrino akıları arasındaki bu ayrılığa " **solar nötrino problemi** " adı verilir.

Çalışmamız, rezonans flavor dönüşümüne dayanarak solar nötrino probleminin mümkün bir çözümü üzerinde olacaktır. Açıkça, problemimiz solar nötrino titreşimine ve rezonans dönüşümüne göre nötrino parametreleri için izin verilen bölgeyi bulmaktır.

Standard Modelde nötrino kütlesizdir. Teoriksel olarak bu yeterli derecede memnun edici değildir. Biz kütleli bir nötrino farzedeceğiz. En azından bir nötrino özdurumu sıfırdan farklı bir kütleye sahip ise ve zayıf etkileşim bozunmalarında yaratılan nötrino durumları serbest Hamiltoniyenin kararlı durumları olmayan tanımlı kütle durumları değillerse nötrino durumları arasında titreşim meydana gelebilir. Özel yüklü leptonlarla zayıf-etkileşim bozunmalarında üretilen nötrino durumları $|\nu_e\rangle$, $|\nu_\mu\rangle$, $|\nu_{tau}\rangle$ **flavor** ya da **akım durumları** olarak adlandırılır. Flavor özdurumları serbest hamiltoniyeni diagonal yapan kütle özdurumlarının lineer birleşimidir. Yani, flavor özdurumları, $|\nu_f\rangle$, iki boyutlu üniter matris $(S(\theta_V)^+ S(\theta_V) = I)$ yardımıyla kütle özdurumlarına dayanarak ifade edilebilir,

$$|\nu_f\rangle = S(\theta_V)|\nu\rangle S(\theta_V) = \begin{pmatrix} \cos\theta_V & \sin\theta_V \\ -\sin\theta_V & \cos\theta_V \end{pmatrix}$$

Burada,

$$|\nu_f\rangle = \begin{pmatrix} |\nu_e\rangle \\ |\nu_f\rangle \end{pmatrix}$$

$$|\nu\rangle = \begin{pmatrix} |\nu_1\rangle \\ |\nu_2\rangle \end{pmatrix}$$

ve θ_V vakum karışım açısını ifade eder.

Solar maddelerdeki nötrinoların üretimi bu maddede yer alan nötrinolar ve elektronlar arasındaki etkileşmeler tarafından tespit edilir. Nötrino titreşimini vakumda ve maddede inceleyeceğiz. Schrödinger denklemine benzer olan hareket denklemi ile Hamiltoniyenden hareket ederek kütlenin karesini ve bir flavor özdurumunun başka bir flavor özdurumuna geçiş ya da bir flavor özdurumunun aynı flavor özdurumunda kalma olasılığını inceleyeceğiz. Bu olasılık vakumda $\sin^2 2\theta_V$, nötrino kütlesinin karesi farkı olarak bilinen $\Delta m^2 = |m_1^2 - m_2^2|$ ve nerjiye bağlıdır. Madde içinde ise bu olasılık aynı zamanda elektron yoğunluğuna bağlı olacaktır. Ayrıca madde içinde vakum karışım açısı ve yoğunluğa bağlı olan yeni bir karışım açısı tanımlanır. Madde içinde yoğunluk sabit ise bu karışım açısıda sabit olacaktır. Yoğunluk değişiyorsa bu karışım açısıda değişecektir. Bizim için önemli olan MSW etkisine göre hesapladığımız ortalama hayatta kalma olasılığıdır. Bu olasılık tabii ki Δm^2, $\sin^2 2\theta_V$ ve enerjiye bağlı olarak değişmektedir. Dikkat etmemiz gereken değerler minimum ve maksimum olasılık değerleri, rezonans durumundaki enerji değeri ve adiabatik durumdaki enerji değeridir. Adiabatik durumda maddedeki karışım açısının türevi ihmal edilebilecek kadar küçüktür. Yani, bir kütle özdurumu başka bir kütle özdurumuna geçmemekte, atlamamaktadır. Eğer enerji adiabatik durumundaki enerjiden daha büyük ise bir kütle özdurumu başka bir kütle özdurumuna geçiş yapmaktadır. Bizim için rezonans ve adiabatik koşulları çok önemlidir. Çünkü nötrino titreşiminin en yoğun olduğu bölgeler bunlardır.

Nötrino parametrelerindeki sınırlar tahmin edilmiş akılara özellikle Boron nötrino akısına (ϕ_B) bağlıdır. Bu akı büyük belirsizliklere sahiptir. Bundan dolayı yeni bir f_B parametresi tanımlanır. Bu parametre orijinal boron akısı ile Standard Solar Model'e göre tahmin edilmiş akının oranıdır. İlk kademede biz f_B'yi bire eşit alacağız. Yani, Standard Solar Model'e göre tahmin edilen akının orijinal Boron akısına tamamen eşit olduğunu düşüneceğiz. Buna göre Δm^2, $\sin^2 2\theta_V$ parametrelerinde sınırlar bulacağız. Eğer tahmin edilmiş boron nötrino akısını deneylerden elde edilen ile karşılaştırırsak deneysel dataların en elverişli durumunu veren üç koşul gözleyebiliriz.

1) Boron nötrino akısı enerji 7 Mev'den büyük oldoğunda yaklaşık olarak $0.41 \times \phi_B^{SSM}$ olmalıdır ve burada Standard Solar Model'e göre tahmin edilmiş akı (ϕ_B^{SSM}) 5.64 $10^6\ cm^{-2}s^{-1}$ eşittir.

2) Standard Solar Model tahminleriyle ilgili olarak kuvvetli bir şekilde bastırılan ^7Be, pep, ^{13}N ve ^{15}O nötrinolarının akıları ihmal edilebilir.

3) pp nötrino akısının bastırma faktörü çok zayıftır.

İlk iki koşul Homestake ve Kamiokande sonuçlarından elde edilebilir. Eğer Boron nötrino akısı için katkıların değerini azaltacak olursak, ^7Be nötrino akısının katkıları artacaktır. Fakat bu Kamiokande sonucu (R_{ν_e}) ile aynı değildir. Üçüncü koşul GALLEX deneyinden gelmektedir. Son iki koşul ve rezonans enerjiden

$$E_{pp}^{max} < E_{rez} < E_{Be}$$

koşulunu yazabiliriz. Bu koşul ve aşağıda verilen rezonans enerji bağıntısından

$$E_{rez} = \frac{\Delta m^2 \cos 2\theta_V}{2\sqrt{2} G_F n_e^{max}}$$

(n_e^{max} güneşin merkez yoğunluğudur.)
Δm^2 deki genel sınırları bulabiliriz:

$$\frac{E_{pp}^{max} 2\sqrt{2} G_F n_e}{\sqrt{1-\sin^2 2\theta_V}} < \Delta m^2 < \frac{E_{Be} 2\sqrt{2} G_F n_e}{\sqrt{1-\sin^2 2\theta_V}}$$

Eğer $\sin^2 2\theta_V$ birden çok daha küçük ise, $\cos 2\theta_V$ yaklaşık olarak bire eşit olacaktır ve rezonans enerji aşağıdaki forma sahip olacaktır:

$$E_{rez} = \frac{\Delta m^2}{2\sqrt{2} G_F n_e^{max}}$$

Bu durumda, Δm^2 deki sınırlar

$$6.49\ 10^{-6} < \Delta m^2 < 1.33\ 10^{-5} \quad eV^2$$

ile verilir.

$\sin^2 2\theta_V$ deki sınırları bulurken iki durum ele alacağız. Bunlar küçük karışım durumunda $\cos 2\theta_V$ yaklaşık olarak bire eşit olacaktır. Bu durumda bastırma faktörü sadece Boron nötrino akısından gelir. Ortalama hayatta kalma olasılığı ($\tilde{P}$) yaklaşık olarak Landau-Zener formülü ile tanımlanabilir. Deneysel datalardan bu olasılığın 0.3 ve 0.5 arasında olduğu görülür. Δm^2 ve $\sin^2 2\theta_V$ arasındaki analitik ilişki ise

$$\sin^2 2\theta_V \approx \frac{\ln \tilde{P}}{\Delta m^2} \frac{E}{l_n}$$

dir. Burada,

$$l_n = \left| \frac{d}{dx} l_n n_e \right|^{-1}$$

olarak tanımlanır. Bu analitik ilişki ve Δm^2 deki genel sınırlarla küçük karışım durumunda izin verilen bir bölge bulacağız.

Büyük karışım durumu için, bastırma faktörü ^7Be ve ^8B akılarından gelir. Bu durumda ortalama hayatta kalma olasılığı yaklaşık olarak enerjiden bağımsız ve $\sin^2\theta_V$ ye eşittir. Bu yaklaşımda, Kamiodande sinyali aşağıdaki formu alır:

$$R_{\nu_e} = f_B \left(\sin^2\theta_V + r(1 - \sin^2\theta_V) \right)$$

Bu formül kullanılarak, $\sin^2 2\theta_V$ deki sınırları

$$0.82 < \sin^2 2\theta_V < 0.99$$

olarak bulabiliriz. Olasılık enerjiye bağlı olmadığından dolayı Homestake sinyalinden

$$Q_{Ar} = f_B P_H Q_{Ar}^{SSM}$$

(P_H Homestake sinyalinde etki bastırma faktörüdür.)
yazabiliriz. Buradan kolayca $\sin^2 2\theta_V$ deki sınırları

$$0.80 < \sin^2 2\theta_V < 0.92$$

olarak elde edebiliriz. Homestake sinyalinden elde edilen sınırlardaki üst limit Kamiokande sinyalinden elde edilen sınırlardakinden daha kuvvetlidir. Eğer Homestake sinyalinden elde edilen sınırları Δm^2 parametresindeki genel sınırlarla birlikte alırsak, bu durum için verilen bölgeyi bulabiliriz.

f_B parametresini bir kabul ederek her iki durum için izin verilen bölgeleri elde ettik. Ama öncede belirttiğimiz gibi Standard Solar Model'e göre tahmin edilmiş boron akısı orijinal boron akısına eşit olmayabilir. Bu durumlarda f_B parametresi birden farklı olacaktır. f_B parametresi azaldıkça küçük karışım durumdaki izin verilen bölge daha küçük $\sin^2 2\theta_V$ değerlerine kayar. Bunun tam tersi f_B parametresi arttıkça büyük karışımdaki bölge küçük vakum açılarına kayar.

CHAPTER 1

EXPERIMENTAL DATA AND SOLAR NEUTRINO PROBLEM

In the first section, we will discuss the solar neutrino spectrum predicted by the Standard Solar Model (SSM) [1]. The content of the second section is the description of the present data from Homestake, Kamiokande, SAGE and GALLEX experiments. In last section, we will compare the predicted flux with the experimental one.

1.1 Solar Neutrino Spectrum

The principal reactions of the pp chain are:

$$(pp) \quad p+p \rightarrow {}^{2}H + e^{+} + \nu_e \quad (q \leq 0.420 MeV)$$

$$(pep) \quad p+e^{-}+p \rightarrow {}^{2}H + \nu_e \quad (q = 1.442 \ \ MeV)$$

$$(hep) \quad {}^{3}He+p \rightarrow {}^{4}He + \nu_e \quad (q \leq 18.773 \ \ MeV)$$

$$({}^{7}Be) \quad {}^{7}Be+e^{-} \rightarrow {}^{7}Li + \nu_e \quad (q = 0.862 \ \ MeV, \ 89.7\%;$$

$$0.384 \ \ MeV, \ 10.3\%)$$

$$({}^{8}B) \quad {}^{8}B \rightarrow {}^{7}Be^{*} + e^{+} + \nu_e \quad (q \leq 15 \ \ MeV)$$

(q is the neutrino energy).

The pp, hep and ${}^{8}B$ reactions produce neutrinos with all energies from zero up to maximal energy that is shown in each case in parentheses; the neutrinos

Table 1.1: Calculated solar neutrino fluxes.

Source	pp	pep	hep	^7Be	^8B	^{13}N	^{15}O	^{17}F
Flux ($cm^{-2}s^{-1}$)	6.02 $\times 10^{10}$	1.42 $\times 10^{8}$	1.24 $\times 10^{3}$	4.57 $\times 10^{9}$	5.64 $\times 10^{6}$	5.78 $\times 10^{8}$	4.90 $\times 10^{8}$	4.83 $\times 10^{6}$

from each of these sources has a different **continuos spectrum**. The pep and ^7Be neutrinos have **well-defined energy lines.**

The neutrinos from the pp reaction are in some sense the "most fundamental", since this reaction initiates the chain that supplies nearly all (about 99%) of the solar luminosity. The pp neutrinos have low energies and therefore it is difficult to detect them.

The easiest neutrinos to detect are the relatively high-energy neutrinos from the hep and ^8B reactions. Unfortunately, neutrinos from both of these sources are scarce, the hep neutrinos being much fewer in number than the rare ^8B neutrinos.

The principal reactions in CNO cycle are :

$$
\begin{aligned}
^{13}N &\rightarrow {}^{13}C + e^+ + \nu_e \quad (q \leq 1.99 \;\; MeV) \\
^{15}O &\rightarrow {}^{15}N + e^+ + \nu_e \quad (q \leq 1.732 \;\; MeV) \\
^{17}F &\rightarrow {}^{17}O + e^+ + \nu_e \quad (q \leq 1.740 \;\; MeV)
\end{aligned}
$$

But the CNO neutrino sources are expected to be difficult to detect because neither the calculated fluxes nor the characteristic energies are large.

The best estimates for each of neutrino fluxes are given in the Table 1.1 [2].

The flux of the neutrinos from the proton-proton reaction is known more accurately than for any other sources; the estimated uncertainty in the pp flux is

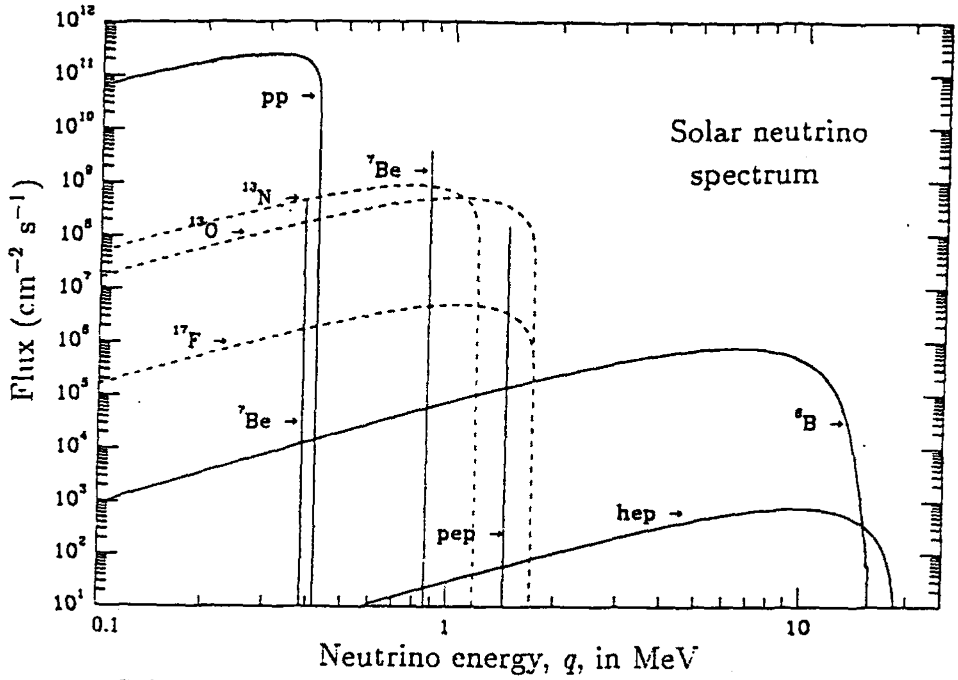

Figure 1.1: Solar neutrino spectrum. This shows the energy spectrum of neutrinos that is predicted by the standard solar model.

only 2%.

Each energy spectrum from a specified solar neutrino source has a characteristic Be-line shape that is pratically independent of the conditions in the solar interior. The pp flux rises slowly with energy and peaks at about 0.31 MeV, then cuts off strongly. The ^8B spectrum, on the other hand, is more nearly symmetric, with a peak at 6.4 MeV and somewhat extended tail. The ^{13}N spectrum, like the pp spectrum, rises slowly and cuts off sharply; the ^{13}N peak is at 0.76 MeV. The solar neutrino spectrum is given in the Figure (1.1).

1.2 Experimental Data

The present data on solar neutrinos come from four experiments : Homestake, Kamiokande, SAGE and GALLEX.

The Homestake signal is about 2.5 SNU[1]. The main part of this signal corresponds to Boron neutrino flux. In this experiment is used a radiochemical chlorine detector to observe electron neutrinos by the reaction:

$$\nu_e + ^{37}Cl \rightarrow e^- + ^{37}Ar \tag{1.1}$$

The threshold energy is 0.814 MeV. The experimental Ar production-rate is [3]:

$$Q_{Ar}^{exp} = 2.55 \pm 0.17(stat) \pm 0.18(syst) \quad SNU \tag{1.2}$$

Boron neutrinos are detected in the Kamiokande experiment, for which the detection threshold is about 7.5 MeV. In the Kamiokande experiment, the electrons are detected by the Čerenkov light that they produce while moving through the water. The signal from this experiment is given in the units $\phi_B^{SSM} \equiv 5.64 \ \ 10^6 \ \ cm^{-1}$ s^{-1} being the prediction in SSM [4]:

$$R_{\nu_e} = \frac{\phi_B^{exp}}{\phi_B^{SSM}} = 0.51 \pm 0.04(stat.) \pm 0.06(syst.) \tag{1.3}$$

There is no direct contradiction between the Homestake and Kamiokande signals. The Boron neutrino flux measured by Kamiokande and that extracted Homestake signal agree within error bars.

The low energy part of the neutrino spectrum is detected by SAGE and GALLEX experiments. In fact, the threshold energy is 0.233 MeV. The Gallium experiments make use of neutrino absorption by gallium:

$$\nu_e + ^{71}Ga \rightarrow e^- + ^{71}Ge \tag{1.4}$$

The average Ge production-rate measured by SAGE and GALLEX experiments are correspondingly [5, 6]:

$$Q_{Ge}^{SAGE} = 69 \pm 11(stat.) \pm 6(syst.) \quad SNU \tag{1.5}$$

$$Q_{Ge}^{GAL} = 79 \pm 10(stat.) \pm 7(syst.) \quad SNU \tag{1.6}$$

We collect all experimental data in the Table (1.2)

[1]1 SNU corresponds to 1 atom produced in 1 sec in 10^{36} target atoms.

Table 1.2: The solar neutrino data used in the analysis.

Experiment	Parameter	Result (1σ)
Homestake	Q_{Ar}^{exp}, SNU	2.55±0.17(stat.)±0.18(syst.)
Kamiokande I+II	$R_{\nu_e} \equiv \frac{\phi_B^{exp}}{\phi_B^{SSM}}$	0.51±0.04(stat.)±0.06(syst.)
GALLEX I+II	Q_{Ge}^{GAL}, SNU	79±10(stat)±7(syst.)
SAGE	Q_{Ge}^{SAGE}, SNU	69±11(stat)±6(syst.)

1.3 Solar Neutrino Problem

The solar neutrino problem can be expressed in the following way. The contributions to the calculated rates in the Homestake experiment is given Table (1.3). Thus the total predicted value of the production-rate is

$$Q_{Ar}^{SSM} = 8.0 \pm 3.0 \quad SNU \tag{1.7}$$

where indicated uncertainty represent the total theoretical range including 3 standard deviation (3σ).

For Gallium experiment the total predicted rate is the following:

$$Q_{Ge}^{SSM} = 131.5\ ^{+21}_{-17} \quad SNU \tag{1.8}$$

where the individual contributions from different fluxes are given in the Table (1.3).

The predicted rates are larger or much larger than observed rates (Q_{Ar}^{exp}, R_{ν_e}, Q_{Ge}^{SAGE}, Q_{Ge}^{GAL}) which we described in previous section (see Table (1.2)). This disagreement between the predicted and the observed rates constitutes the **solar neutrino problem.**

Table 1.3: Individual neutrino contributions to the calculated event rates in the chlorine and gallium solar neutrino experiments.

Neutrino source	Cl (SNU)	Ga (SNU)
pp	0.0	70.8
pep	0.2	3.1
^{7}Be	1.2	35.8
^{8}B	6.2	13.8
^{13}N	0.1	3.0
^{15}O	0.3	4.9
Total	8.0±3.0	131.5^{+21}_{-17}

The discrepancy between calculation and observation is confirmed by Kamiokande II-III signal (see Table (1.2)).

There is no generally accepted solution to the problem although a number of solutions is proposed.

The central question for solar neutrino research can be formulated as follows: Is the solar neutrino problem caused by lack of understanding of the interior of the Sun or it is due to neutrino properties which are not described by the Standard Model?

We would like to explore the properties of neutrinos beyond electroweak standard model. We will assume that neutrino has non zero mass and this gives rise to the neutrino oscillation. In the next chapter, we will discuss this important phenomenon.

CHAPTER 2

NEUTRINO OSCILLATON AND RESONANT CONVERSION

In the Standard Model, neutrino is massles. From a theoretical point of view, this is not satisfactory, because this does not follow from fundamental symmetries. We will assume a massiveness of neutrino. Oscillation between neutrino states can occur if at least one neutrino eigenstate has a non zero mass and if the neutrino states that are created in weak interaction decays are not states of definite mass, that is, not stationary states of the free Hamiltonian. The neutrino states, $|\nu_e\rangle, |\nu_\mu\rangle, |\nu_\tau\rangle$, that are produced in the weak-interaction decays in association with particular charged leptons are called **flavor** or **current eigenstates**. The flavor eigenstates are linear combinations of the **mass eigenstates**, the states that do diagonalize the free Hamiltonian.

The solar neutrinos are produced in the center of the Sun by nuclear reactions. The propagation of the neutrinos in the solar matter is determined by the interaction between the neutrinos and electrons presents in this matter [10]. The result of this interaction has at some conditions the form of resonance (MSW) effect [7].

Now, let us discuss neutrino oscillation in vacuum and in matter.

2.1 Neutrino Oscillation In Vacuum

2.1.1 Neutrino Eigenstates

The flavor eigenstates $(\nu_e, \nu_\mu, \nu_\tau)$ can be expressed as linear combinations of the mass eigenstates (ν_1, ν_2, ν_3).

The most important aspects of neutrino oscillations can be understood by studying the explicit solution for two neutrino species. For this two-flavor problem, the flavor eigenstates, $|\nu_f\rangle$, are expressed in terms of the mass eigenstates, $|\nu\rangle$, with the aid of two-dimensional unitary matrix $(S(\theta_V)^+ \, S(\theta_V) = I)$,

$$|\nu_f\rangle = S(\theta_V)|\nu\rangle \tag{2.1}$$

where

$$S(\theta_V) = \begin{pmatrix} \cos\theta_V & \sin\theta_V \\ -\sin\theta_V & \cos\theta_V \end{pmatrix}$$

$$|\nu_f\rangle = \begin{pmatrix} |\nu_e\rangle \\ |\nu_\mu\rangle \end{pmatrix}$$

$$|\nu\rangle = \begin{pmatrix} |\nu_1\rangle \\ |\nu_2\rangle \end{pmatrix}$$

Here, θ_V denotes the vacuum mixing angle. If the energy of the neutrino is large $(E \gg m_1, m_2)$, then the amplitudes of the $|\nu_1\rangle$ and $|\nu_2\rangle$ waves are fixed by the coefficients in equation(2.1). For $|\nu_e\rangle$, they are $\cos\theta_V$ and $\sin\theta_V$, respectively. Moreover, the $|\nu_1\rangle$ and $|\nu_2\rangle$ waves are in phase $(\Delta\varphi = 0)$. In the $|\nu_\mu\rangle$ state, the waves $|\nu_1\rangle$ and $|\nu_2\rangle$ have amplitudes $\sin\theta_V$ and $\cos\theta_V$ and opposite phases: $\Delta\varphi = \pi$ (minus sign in front of $|\nu_1\rangle$.)

So mixed $|\nu_e\rangle$ and $|\nu_\mu\rangle$ are distinguished by a) amplitudes of $|\nu_1\rangle$ and $|\nu_2\rangle$ and b) phase differences between $|\nu_1\rangle$ and $|\nu_2\rangle$ waves.

In the case of maximal mixing $(\theta_V = 45°)$ admixtures of $|\nu_1\rangle$ and $|\nu_2\rangle$ are equal to $|\nu_e\rangle$ and $|\nu_\mu\rangle$ are distinguished by phase difference only. Without loss of generality we can choose $0 \leq \theta_V \leq \frac{\pi}{4}$ so that $|\nu_e\rangle$ is "mostly" $|\nu_1\rangle$.

2.1.2 Evolution Equation And Its Solution

The time development of the flavor eigenstates in vacuum is described by an equation that is analogous to the Schrödinger equation:

$$\begin{aligned} i\frac{d}{dt}|\nu_f\rangle &= H|\nu_f\rangle \\ H &\cong \frac{M^2}{2E} \end{aligned} \tag{2.2}$$

where H is the Hamiltonian for ultrarelativistic neutrino, E is the energy of neutrino, M^2 is the vacuum mass matrix squared. This equation is called "evolution equation".

Let us now write evolution equation for mass eigenstates[1].

$$\begin{aligned} i\frac{d}{dt}|\nu\rangle &= H|\nu\rangle \\ H^{diag} &= S(\theta_V)^{+}HS(\theta_V) = \begin{pmatrix} H_1 & 0 \\ 0 & H_2 \end{pmatrix} \end{aligned} \tag{2.3}$$

where $H_i \equiv \frac{m_i^2}{2E}$ are the eigenvalues of the Hamiltonian. By using equation (2.1), we obtain M^2 as the following,

$$M^2 = \pm\frac{\Delta m^2}{4E}\begin{pmatrix} -\cos 2\theta_V & \sin 2\theta_V \\ \sin 2\theta_V & \cos 2\theta_V \end{pmatrix}$$

where $\Delta m^2 = |m_1^2 - m_2^2|$ is the neutrino mass squared difference. The plus sign applies if $m_2 > m_1$ and the minus sign in the opposite case.

The solution of evolution equation or the time evolution of an electron-neutrino state is expressed as

$$|\nu_e\rangle_t = \cos\theta_V e^{(-iH_1 t)}|\nu_1\rangle + \sin\theta_V e^{(-iH_2 t)}|\nu_2\rangle \tag{2.4}$$

[1] Mass eigenstates are orthogonal: $\langle\nu_i|\nu_j\rangle = \delta_{ij}$

The probability amplitude for an electron neutrino remaining an electron neutrino after traveling for a time t is

$$\langle \nu_e | \nu_e \rangle_t = \cos^2 \theta_V e^{(-iH_1 t)} + \sin^2 \theta_V e^{(-iH_2 t)} \tag{2.5}$$

which gives a probability of a ν_e remaining a ν_e

$$|\langle \nu_e | \nu_e \rangle_t|^2 = 1 - \sin^2 2\theta_V \sin^2 \left(\frac{H_2 - H_1}{2} t \right) \tag{2.6}$$

The two mass eigenstates are assumed to have the same momentum, which implies that they have slightly different energies if they have finite masses. The energy difference for relativistic neutrinos is:

$$H_2 - H_1 = \frac{m_2^2 - m_1^2}{2E} = \pm \frac{\Delta m^2}{2E} \tag{2.7}$$

The survival probability for electron neutrino may be written therefore in the following form

$$|\langle \nu_e | \nu_e \rangle_t|^2 = 1 - \sin^2 2\theta_V \sin^2 \left(\frac{\pi R}{L_V} \right) \tag{2.8}$$

where R is the distance traveled in a time t and L_V is the vacuum oscillation lenght, the distance over which the neutrino returns to the initial state (condition: $\Delta\varphi(L_V) = 2\pi$). This quantity can be written in the form

$$L_V \equiv \frac{4\pi E}{\Delta m^2}. \tag{2.9}$$

The probability[2] to observe the muon flavor, $|\nu_\mu\rangle$, is

$$|\langle \nu_\mu | \nu_e \rangle_t|^2 = \sin^2 2\theta_V \sin^2 \left(\frac{\pi R}{L_V} \right) \tag{2.10}$$

Also the probability of a $|\nu_\mu\rangle$ neutrino to be observed as an electron neutrino is the same as the reverse process

$$|\langle \nu_e | \nu_\mu \rangle_t|^2 = |\langle \nu_\mu | \nu_e \rangle_t|^2 \tag{2.11}$$

[2]The total probability is normalized: $|\langle \nu_e | \nu_e \rangle_t|^2 + |\langle \nu_\mu | \nu_e \rangle_t|^2 = 1$

The magnitude of vacuum mixing described by $\sin^2 2\theta_V$, is expected to be small because the possibly analogous quark mixing angles are small.

To observe variations of flux flavor with distance or time due to neutrino oscillations, a neutrino source must be localized within a region that is much smaller than L_V. Therefore, by the uncertainty principle, the neutrino wave function has a spread of momenta, $\triangle \geq \frac{\hbar}{L_V}$.

Let us discuss neutrino oscillation in matter. Mixing angle, H_1 and H_2 will depend on the density.

2.2 Neutrino Oscillation In Matter

2.2.1 Evolution Equation

The evolution equation for the flavor eigenstates in matter is [9]:

$$\begin{aligned} i\frac{d}{dt}|\nu_f\rangle &= H|\nu_f\rangle \\ H &= \frac{M^2}{2E} + V \\ |\nu_f\rangle &= \begin{pmatrix} |\nu_e\rangle \\ |\nu_\mu\rangle \end{pmatrix} \end{aligned} \tag{2.12}$$

where V describes matter (refraction) effect, was derived first by Wolfenstein (1978, 1979) [7]. In the Standard Model, V is diagonal and can be written as

$$V = \begin{pmatrix} \sqrt{2}G_F n_e & 0 \\ 0 & 0 \end{pmatrix},$$

where G_F is the Fermi constant and n_e is the electron number density. The value of the V is determined by the neutrino-electron scattering.

Mixing angle (θ_m) and neutrino eigenstates $|\nu_{im}\rangle$ $(i = 1, 2)$ in matter are the generalizations of θ_V and $|\nu_i\rangle$ $(i = 1, 2)$. Eigenstates $|\nu_{im}\rangle$ are determined as the states which diagonalize the Hamiltonian (2.12):

$$|\nu_f\rangle = S(\theta_m)|\nu_m\rangle$$

$$
\begin{aligned}
S(\theta_m) &= \begin{pmatrix} \cos\theta_m & \sin\theta_m \\ -\sin\theta_m & \cos\theta_m \end{pmatrix} \\
H^{diag} &= S(\theta_m)^{+} H S(\theta_m)
\end{aligned} \tag{2.13}
$$

By using equation (2.13) and some trigonometric relations, the first equation (2.12) can be written as

$$
i\frac{d}{dt}|\nu_f\rangle = \pm\frac{\Delta_m}{2}\begin{pmatrix} -\cos 2\theta_m & \sin 2\theta_m \\ \sin 2\theta_m & \cos 2\theta_m \end{pmatrix}|\nu_f\rangle \tag{2.14}
$$

The explicit form for Δ_m is

$$
\begin{aligned}
\Delta_m &= [(\pm\,\Delta_V \cos 2\theta_V - \sqrt{2}G_F n_e)^2 + (\Delta_V \sin 2\theta_V)^2]^{\frac{1}{2}} \\
\Delta_V &= \frac{\Delta m^2}{2E}
\end{aligned} \tag{2.15}
$$

The plus sign applies for $m_2 > m_1$ and the minus sign for $m_1 > m_2$.

Since H is the function of θ_V, $\frac{E}{\Delta m^2}$, and n_e, the mixing angle in matter will also depend on these quantities as determined explicitly by the relation

$$
\begin{aligned}
\sin 2\theta_m &= \frac{\sin 2\theta_V}{D_m} \\
D_m &= \left(1 - 2\frac{L_V}{L_e}\cos 2\theta_V + \left(\frac{L_V}{L_e}\right)^2\right)^{\frac{1}{2}}
\end{aligned} \tag{2.16}
$$

where L_e is the neutrino-electron refraction length that is defined by

$$
L_e = \frac{\sqrt{2}\pi}{G_F n_e} \tag{2.17}
$$

This is independent of energy, unlike the oscillation lengths in vacuum or in matter.

By using the equations (2.13) and (2.12), we can obtain the evolution equation for the eigenstates:

$$
i\frac{d}{dt}\begin{pmatrix} |\nu_{1m}\rangle \\ |\nu_{2m}\rangle \end{pmatrix} = (H^{diag} - iS(\theta_m)^{+}\frac{d}{dt}S(\theta_m))\begin{pmatrix} |\nu_{1m}\rangle \\ |\nu_{2m}\rangle \end{pmatrix} \tag{2.18}
$$

Explicitly the equation (2.18) can be written as

$$
\begin{aligned}
i\frac{d}{dt}\begin{pmatrix} |\nu_{1m}\rangle \\ |\nu_{2m}\rangle \end{pmatrix} &= \begin{pmatrix} H_{1m} & -i\dot{\theta}_m \\ i\dot{\theta}_m & H_{2m} \end{pmatrix}\begin{pmatrix} |\nu_{1m}\rangle \\ |\nu_{2m}\rangle \end{pmatrix} \\
\dot{\theta}_m &\equiv \frac{d\theta_m}{dt}
\end{aligned} \tag{2.19}
$$

The solution of the evolution equation in matter is expressed:

$$|\nu_e\rangle_t = \cos\theta_m^{\circ} e^{-i\int H_{1m}dt}|\nu_{1m}\rangle + \sin\theta_m^{\circ} e^{-i\int H_{2m}dt}|\nu_{2m}\rangle \tag{2.20}$$

where θ_m° is the mixing angle in the production point. The probability amplitude for an electron neutrino remaining an electron neutrino after traveling for a time t is:

$$\langle\nu_e|\nu_e\rangle_t = \cos\theta_m^{\circ}\cos\theta_m e^{-i\int H_{1m}dt} + \sin\theta_m^{\circ}\sin\theta_m e^{-i\int H_{2m}dt} \tag{2.21}$$

Here $\theta_m = \theta_m(t)$

2.2.2 Resonance Condition

The resonant character of matter oscillations can be seen from (2.16) for $\sin 2\theta_m$. If $m_2 \geq m_1$, then $\sin 2\theta_m$ is maximal ($\sin 2\theta_m = 1$) at

$$\left(\frac{L_V}{L_e}\right)_{res} = \cos 2\theta_V \tag{2.22}$$

which is often referred to as the resonance condition.

There is no resonance for electron neutrinos if $m_2 < m_1$. (In this case there would be a resonance for $\bar{\nu}_e$). We assume $m_2 > m_1$.

At the resonant density, the two diagonal elements of Hamiltonian (2.12) are equal.

By subsituting L_V and L_e from equations (2.9) and (2.17) the **MSW resonance density** can be written as

$$n_{e,res} = \frac{\Delta m^2 \cos 2\theta_V}{2\sqrt{2}G_F E_{res}} \tag{2.23}$$

For small mixing in vacuum $\sin^2 2\theta_m$ is of order of unit in narrow region around $n_{e,res}$. Beyond this region $\sin^2 2\theta_m$ becomes small ($\sin^2 2\theta_m \ll 1$). The interval

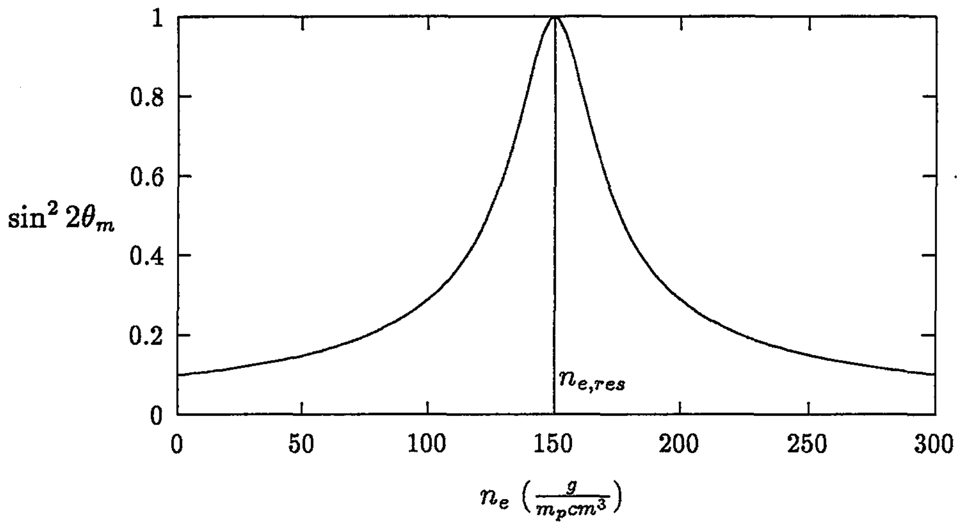

Figure 2.1: The dependence of $\sin^2 2\theta_m$ on effective density of matter ($sin^2 2\theta_V = 0.1$, $\Delta m^2 = 10^{-4}\ eV^2$, $E_{res} = 4.533$ MeV).

of densities $\Delta n_{e,res}$ in which $\sin^2 2\theta_m > \frac{1}{2}$ is called the width of resonant layer. From equation (2.16) one obtains

$$\triangle\, n_{e,res} = n_{e,res} \tan 2\theta_V \tag{2.24}$$

The θ_m angle depends on n_e. In terms of $n_{e,res}$ it can be represented as follows (see Figure (2.1)):

$$\sin 2\theta_m = \frac{\tan 2\theta_V}{\left(\left(1 - \frac{n_e}{n_{e,res}}\right)^2 + \tan^2 2\theta_V\right)^{\frac{1}{2}}} \tag{2.25}$$

$$\theta_m = \begin{cases} \frac{\pi}{2} & n_e \gg n_{e,res} \\ \frac{\pi}{4} & n_e = n_{e,res} \\ \theta_V & n_e \ll n_{e,res} \end{cases}$$

When the density decreases from large values $n_e \gg n_{e,res}$ to zero the mixing angle in matter changes from $\frac{\pi}{2}$ to $\theta_m = \theta_V$. The eigenstates in matter rotate with respect to the eigenstates of weak interaction on the angle $\frac{\pi}{2}$. This means that if at $n_e \gg n_{e,res}$ some eigenstate $|\nu_{im}\rangle$ coincides with $|\nu_e\rangle$ then at $n_e \ll n_{e,res}$ it will approach to $|\nu_\mu\rangle$.

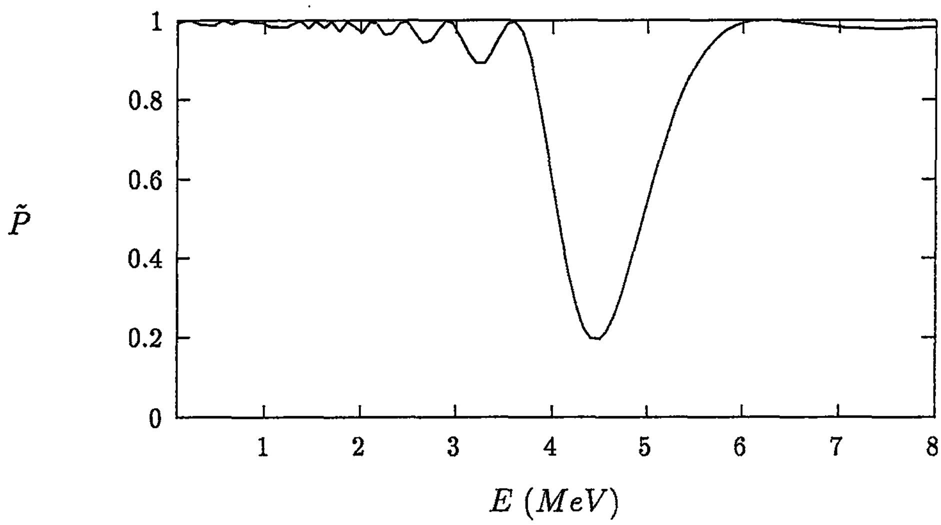

Figure 2.2: The survival probability after crossing the layer of medium with constant density ($sin^2 2\theta_V = 0.1$, $\Delta m^2 = 10^{-4}\ eV^2$, distance traveled $R = 10^7$ km).

2.2.3 Oscillations In Matter With Constant Density

In this case density $n_e = const$, $\theta_m = const$, $\dot{\theta_m} = 0$ and as in vacuum case the equations for the eigenstates $|\nu_{1m}\rangle$ and $|\nu_{2m}\rangle$ are splitted. The $|\nu_{im}\rangle$ evolve independently; there are no $|\nu_{1m}\rangle \longleftrightarrow |\nu_{2m}\rangle$ transitions, and both flavors and admixtures of $|\nu_{im}\rangle$ are determined by θ_m.

The difference between the energy eigenvalues for the two mass eigenstates is

$$H_{1m} - H_{2m} = \Delta_m = \Delta_V\ D_m \tag{2.26}$$

where Δ_V and D_m are defined in section 2.2.1.

The probability that an electron neutrino remains an electron neutrino has the same algebraic form as for vacuum oscillations, (see Figure(2.2)), that is

$$|\langle\nu_e|\nu_e\rangle_t|^2 = 1 - \sin^2 2\theta_m \sin^2\left(\frac{\pi R}{L_m(E)}\right) \tag{2.27}$$

The probability of being observed as a neutrino of a different flavor is

$$|\langle\nu_\mu|\nu_e\rangle_t|^2 = \sin^2 2\theta_m \sin^2\left(\frac{\pi R}{L_m(E)}\right) \tag{2.28}$$

where $L_m(E) = L_V/D_m$.

At the resonance density, $\left(\frac{L_V}{L_e}\right)_{res} = \cos 2\theta_V$, $(D_m)_{res} = \sin 2\theta_V$ and $(\sin 2\theta_m)_{res} = 1$ or $\theta_m = \frac{\pi}{4}$.

At very high electron densities, the matter mixing angle approaches $\frac{\pi}{2}$.

We saw that the solution is the same as in vacuum: the propagation has a character of oscillations. The only difference is that now the parameters of oscillations (depth, length) are determined by the matter mixing angle (θ_m) and by the difference of the eigenvalues in matter, $H_2 - H_1$. Since these values depend on the density and the neutrino energy and differ from the vacuum values, the oscillation parameters will differ from those in vacuum. These oscillations may be realized for neutrinos propagation inside the Earth.

2.2.4 Oscillation In Matter With Varying Density

The mixing angle θ_m changes along the neutrino trajectory and this change has two crucial consequences [8]:

i) As θ_m determines the flavor composition of the neutrino eigenstates according to equation (2.13), the change of θ_m means the change of flavor of the eigenstates.

At small density, the electron neutrino almost coincides, for small vacuum mixing angles, with the lower mass eigenstate $|\nu_{1m}\rangle$ and the second flavor $|\nu_\mu\rangle$ eigenstate approximately coincides with the mass eigenstate $|\nu_{2m}\rangle$. The mass of the lowest mass eigenstates increases monotonically with ambient electron density and becomes asymptotically proportional to the electron density. If $m_2 \geq m_1$,

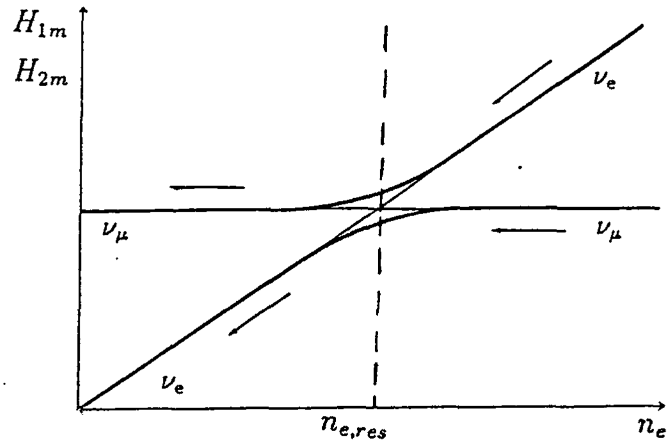

Figure 2.3: The dependence of eigenvalues on density.

then at large electron densities the heavier mass eigenstate, $|\nu_{2m}\rangle$, becomes close to $|\nu_e\rangle$ and the lowest mass eigenstate, $|\nu_{1m}\rangle$, remains essentially unchanged as a function of electron density. An electron neutrino that is created in the solar interior moves from high densities to lower densities (see Figure (2.3)).

ii) $\dot{\theta_m}$ is not zero; the equations for the eigenstates are not splitted, there are transitions between the eigenstates ($|\nu_{1m}\rangle \longleftrightarrow |\nu_{2m}\rangle$).

If the electron density changes at a sufficiently slow rate so that

$$|\dot{\theta_m}| \ll |H_1 - H_2| \tag{2.29}$$

then in the first approximation we can neglect $\dot{\theta_m}$ in the evolution equation (2.19) [10]. The condition (2.29) is called **the adiabaticity condition**. In the adiabatic approximation the transitions $|\nu_{1m}\rangle \longleftrightarrow |\nu_{2m}\rangle$ are neglected, and as in the cases of vacuum and uniform matter density the eigenstates propagate independently. Suppose the electron neutrino is produced at some density n_e°, then the neutrino state in arbitrary moment t can be written as

$$|\nu\rangle_t = \cos\theta_m^\circ \psi_1(t)|\nu_{1m}\rangle + \sin\theta_m^\circ \psi_2(t)|\nu_{2m}\rangle \tag{2.30}$$

where $\psi_i(t) = \exp\left(-i\int_t^{t_f} H_{im}(t')dt'\right) = e^{(-i\varphi_i)}(i = 1, 2)$; are the solutions of the evolution equation, θ_m° is the mixing angle in the production point. In constrast with vacuum and uniform matter cases, now the flavor compositions of eigenstates

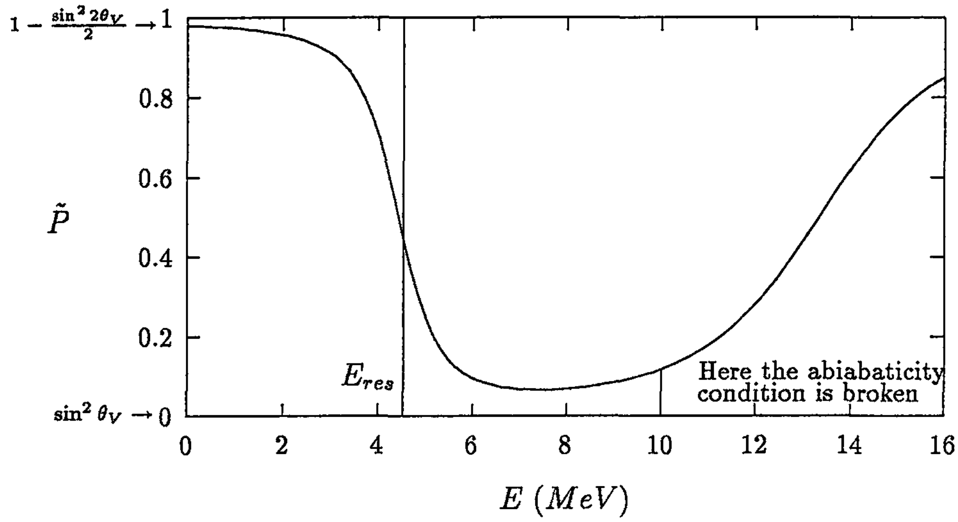

Figure 2.4: The average survival probability in varying density ($sin^2 2\theta_V = 0.04$, $\Delta m^2 = 10^{-4}\ eV^2$).

change according to density change.

The amplitude of probability to find the electron neutrino in some other point is:

$$\langle \nu_e | \nu \rangle_t = \cos\theta_m \cos\theta_m^\circ + \sin\theta_m \sin\theta_m^\circ \exp(-i(\varphi_2 - \varphi_1)) \tag{2.31}$$

The average survival probability (see Figure (2.4)) is as

$$\tilde{P} = |\langle \nu_e | \nu_e \rangle_t|^2 = \frac{1}{2}(1 + \cos 2\theta_m \cos 2\theta_m^\circ) \tag{2.32}$$

The adiabaticity condition has a very simple form at resonance (moreover it is at resonance this condition is the most crucial):

$$\begin{aligned} 2 \triangle r_{res} &\geq L_{m,res} \\ \Delta r_{res} &= \left| \frac{dn_e}{dr} \right|^{-1} \triangle n_{e,res} = l_n \tan 2\theta_V \end{aligned} \tag{2.33}$$

where $l_n \equiv \left| \frac{d \ln n_e}{dr} \right|^{-1}$, Δr_{res} is the spatial half width of the resonant layer and $L_{m,res}$ is the matter oscillation length at resonance. According to (2.33) at least one oscillation length should be obtained in the resonant layer. Condition (2.33) permits the introduction of the adiabaticity parameter:

$$\kappa_{res} = \frac{\triangle r_{res}}{L_{m,res}} = \frac{l_n \sin^2 2\theta_V}{L_V \cos 2\theta_V} \tag{2.34}$$

which determines the degree of adiabaticity violation. At $\kappa \geq \frac{1}{2}$ oscillations occur in the adiabatic regime. The adiabaticity condition determines the energy E_{na} which can be obtained from $\kappa \geq \frac{1}{2}$ as

$$E_{na} = \frac{l_n \sin^2 2\theta_V \triangle m^2}{cos 2\theta_V} \tag{2.35}$$

So that at $E > E_{na}$ the adiabaticity condition is broken. If the adiabaticity condition is broken in some region then the transitions $|\nu_{1m}\rangle \longleftrightarrow |\nu_{2m}\rangle$ become essential. Now, $\dot{\theta}_m$ is not zero. The adiabaticity violation will take place in resonance layer. In this case, before resonance and after resonance we do not have adiabaticity violation but around resonance we have. The neutrino eigenstates after crossing the resonance can be written as a superposition of $|\nu_1\rangle_t$ and $|\nu_2\rangle_t$ eigenstates [11]:

$$\begin{aligned} |\nu_e\rangle_t = \cos\theta_V & \left(a_1 \cos\theta_m e^{i\int_t^{t_r} H_{1m}(t')dt'} - a_2^* \sin\theta_m e^{i\int_t^{t_r} H_{2m}(t')dt'}\right) e^{-i\int_{t_r}^{t_f} H_{1m}(t')dt'} |\nu_1\rangle_{t_{res}} \\ + \sin\theta_V & \left(a_1^* \sin\theta_m e^{i\int_t^{t_r} H_{2m}(t')dt'} + a_2 \cos\theta_m e^{i\int_t^{t_r} H_{1m}(t')dt'}\right) e^{-i\int_{t_r}^{t_f} H_{2m}(t')dt'} |\nu_2\rangle_{t_{res}} \end{aligned}$$

The average survival probability can be then obtained as

$$\tilde{P} = |\langle\nu_e|\nu_e\rangle_t|^2 = \frac{1}{2} + \left(\frac{1}{2} - P_x\right) \cos 2\theta_m \cos 2\theta_V^\circ \tag{2.36}$$

where $P_x = |a_2|^2$ is the probability of transition from $|\nu_2\rangle_t$ to $|\nu_1\rangle_t$ during resonance crossing. To calculate the probability P_x, we can make the approximation that the density of electrons varies lineraly in the transition region. That is, a Taylor-series expansion is made about the resonance position and the second and higher derivative terms are discarded:

$$n_e(t) \approx n_e(t_r) + \left.\frac{dn_e}{dt}\right|_{t_r} (t - t_r)$$

In this approximation the probability of transition between $|\nu_1\rangle_t$ and $|\nu_2\rangle_t$ can be calculated by using the **Landau-Zener** formula [11]. This is achieved by solving the Schrödinger equation exactly in this limit. Application of the Landau-Zener result to the current situation gives

$$P_x = P_{LZ} = e^{\left(-\frac{E_{na}}{E}\right)} \tag{2.37}$$

where E_{na} is defined in (2.35)

Adiabaticity violation usually weakens the flavor conversion so that for very strong violation the flavor is not changed.

CHAPTER 3

BOUNDS ON THE NEUTRINO PARAMETERS

In this chapter, we are going to confront the predictions of the **MSW theory** with experimental results. We will find the constraints on Δm^2 and $\sin^2 2\theta_V$. The parameter f_B will be introduced which takes in account the rather large uncertainties in predictions of the original Boron neutrino flux, ϕ_B. The treatment will be different for small or large mixing. First, we will get three conditions from experimental quantities (R_{ν_e}, Q_{Ar}^{exp}, Q_{Ge}^{SAGE}, Q_{Ge}^{GAL}) defined in the first chapter. Then, we will discuss the small and large mixing cases.

3.1 Bounds On Neutrino Fluxes From Experimental Data

The bounds on neutrino parameters depend on the predicted fluxes, especially on the original Boron neutrino flux, ϕ_B. As we told above, this flux has large uncertainties, mainly due to poorly known nuclear cross section at low energies, as well as to astrophysical uncertainties which influence the temperature of the Sun. For this reason, we will discuss the MSW effect without referring to the SSM Boron neutrino flux.

The best fit of experimental data gives the following values of neutrino fluxes [2, 13]:

i) The Boron neutrino flux should be $\sim 0.41\phi_B^{SSM}$ at $E > 7$ MeV, where $\phi_B^{SSM} = 5.64\ \ 10^6\ \ cm^{-2}\,s^{-1}$ is the SSM value.

ii) The fluxes of the ^7Be, pep, ^{13}N and ^{15}O neutrinos are strongly suppressed with respect to the SSM predictions and can be neglected

iii) The suppression of the pp neutrino flux is very weak.

The first two conditions can be extracted from Homestake and Kamiokande results: if we will decrease the value of the contribution for the Boron neutrino flux, the contribution of the ^7Be neutrino flux will increase. But this does not agree with Kamiokande result, R_{ν_e} [7]. The third condition follows from the GALLEX experiment in which the Ge production-rate can be written as

$$Q_{Ge} = Q^{SSM}_{Ge,pp} + 0.41 Q^{SSM}_{Ge,B} \approx 77\ SNU \tag{3.1}$$

where $Q^{SSM}_{Ge,pp} = 71\ SNU$ and $Q^{SSM}_{Ge,B} = 14\ SNU$.

The original Boron neutrino flux can be written as

$$\phi_B = f_B \phi_B^{SSM} \tag{3.2}$$

where f_B is the parameter mentioned above.

It is usefull to introduce the **effective suppression factors** for B-neutrinos

$$P_i \approx \frac{\int dE \phi_B^{SSM} \sigma_i \tilde{P}}{\int dE \phi_B^{SSM} \sigma_i}\ ,\quad (i = H, K) \tag{3.3}$$

for Homestake (P_H) and for Kamiokande (P_K). In the formula (3.3), $\tilde{P}$ is the survival probability which we calculated in second chapter, equation (2.36), E is the neutrino energy and σ_i are the cross sections,

$$\sigma_H = \sigma_{Ar}(E)\ \ ,\ \ \sigma_K = \int dT_e W(T_e) \frac{\sigma_{\nu_e e}(E, T_e)}{dT_e}$$

where T_e is the energy of the recoil electrons and $W(T_E)$ describes the efficiency of the recoil-electron registration in Kamiokande, as well as the energy resolution of the detector. Since the survival probability depends on the neutrino parameters, also the suppression factors, P_i, strongly depend on these parameters. Table (3.1) shows the suppression factors for different $\sin^2 2\theta_V$ and fixed $\triangle m^2$. From

Table 3.1: The effective survival probabilities for Boron neutrinos in Homestake P_H and the Kamiokande P_K experiments for different values of $\sin^2 2\theta$ and $\Delta m^2 = 6\ 10^{-6} eV^2$ [2].

$\sin^2\theta_V$	$1.25\ 10^{-3}$	$2\ 10^{-3}$	$5\ 10^{-3}$	$7\ 10^{-3}$	10^{-2}	$2\ 10^{-2}$	$3\ 10^{-2}$
P_H	0.824	0.734	0.465	0.345	0.222	0.0564	0.0220
P_K	0.834	0.749	0.487	0.366	0.240	0.0630	0.0220
P_H/P_K	0.988	0.980	0.955	0.943	0.925	0.895	0.914

this table we can also see that the ratio $\frac{P_H}{P_K}$ is close to 1 and changes with $\sin^2 2\theta_V$ rather weakly.

We can write the signals of the solar neutrino experiments in terms of f_B and P_i. The Homestake experiment gives the ^{37}Ar production-rate which can be written as

$$Q_{Ar} = f_B P_H Q_{Ar,B}^{SSM} + Q_{Ar}^{oth} \tag{3.4}$$

where

$$Q_{Ar,B}^{SSM} = \int dE \phi_B^{SSM} \sigma_H = 6.2\ SNU \tag{3.5}$$

is the SSM contribution of Boron neutrinos and Q_{Ar}^{oth} is the contribution of all the other fluxes. We can introduce the ratio between the real ^{37}Ar production-rate and the predicted one from SSM:

$$R_{Ar} \equiv \frac{Q_{Ar}}{Q_{Ar}^{SSM}} = f_B P_H k_B + \frac{Q_{Ar}^{oth}}{Q_{Ar}^{SSM}}, \tag{3.6}$$

where $Q_{Ar}^{SSM} = 8.0\ \ SNU$ and $k_B \equiv \frac{Q_{Ar,B}^{SSM}}{Q_{Ar}^{SSM}} = 0.775$ is the part of the Boron neutrinos in the total signal according to the SSM.

In the Kamiokande experiment we have the contribution from neutral current $\nu_\mu(\nu_\tau)-e$ scattering. Due to this effect, the signal in Kamiokande can be expressed as

$$R_{\nu_e} = f_B(P_K + r(1 - P_K)) \tag{3.7}$$

where the ratio of the $\nu_\mu(\nu_\tau) - e$ and $\nu_e - e$ cross sections, is $r \approx 0.16$.

Let us introduce **double ratio** of suppresion factors from the equations (3.6) and (3.7):

$$R_{H/K} \equiv \frac{R_{Ar}}{R_{\nu_e}} = \frac{f_B P_H k_B + \frac{Q_{Ar}^{oth}}{Q_{Ar}^{SSM}}}{f_B[P_K + r(1 - P_K)]} \tag{3.8}$$

From existing experimental data Table (1.2) one finds:

$$R_{H/K} = 0.625 \pm 0.11(1\sigma) \tag{3.9}$$

3.2 General Constraint On Δm^2

The second and third conditions from section 3.1 give rise to a constraint on the mass difference, Δm^2, which is valid for large range of the parameter $\sin^2 2\theta_V$. In the frame work of MSW theory, these two conditions can be expressed as the following:

$$E_{pp}^{max} < E_{res} < E_{Be} \tag{3.10}$$

where $E_{pp}^{max} = 0.42MeV$ is the maximal value of pp neutrinos, $E_{Be} = 0.86MeV$ is the ^7Be energy line and E_{res} is the energy of the adiabatic edge which is determined by resonance condition in the center of the Sun:

$$E_{res} = \frac{\Delta m^2 \cos 2\theta_V}{2\sqrt{2} G_F n_e^{max}} \tag{3.11}$$

where n_e^{max} is the central density of the Sun. The condition (3.10) and the equation (3.11) give:

$$\frac{E_{pp}^{max} 2\sqrt{2} G_F n_e}{\sqrt{1 - \sin^2 2\theta_V}} < \Delta m^2 < \frac{E_{Be} 2\sqrt{2} G_F n_e}{\sqrt{1 - \sin^2 2\theta_V}} \tag{3.12}$$

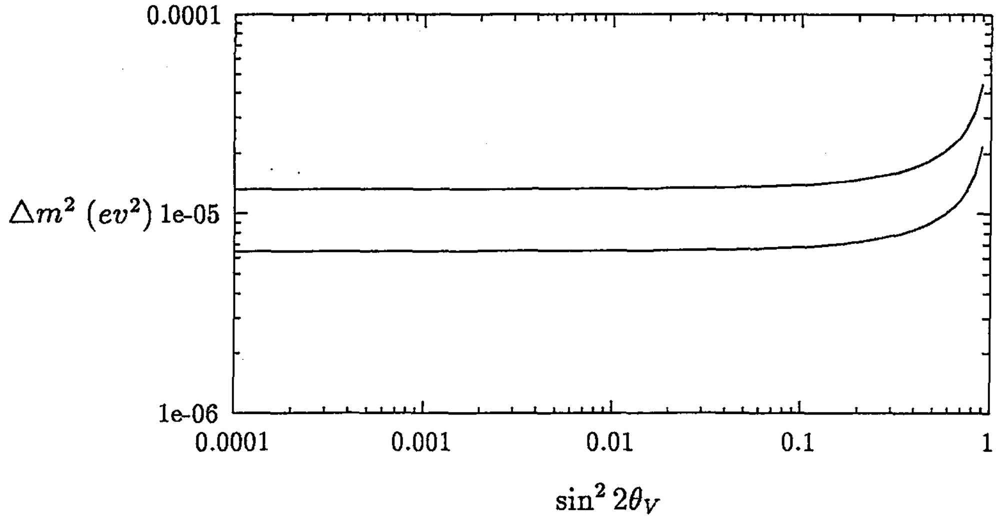

Figure 3.1: General constraint on Δm^2.

and it is shown in Figure 3.1.

If $\sin^2 2\theta_V \ll 1$, we can put $\cos 2\theta_V \approx 1$ and the resonant energy have in the following form:

$$E_{res} = \frac{\Delta m^2}{2\sqrt{2} G_F n_e^{max}} \tag{3.13}$$

In this case, the bound on Δm^2 is given by

$$6.49 \ \ 10^{-6} < \Delta m^2 < 1.33 \ \ 10^{-5} \quad eV^2 \tag{3.14}$$

3.3 Small Mixing Solution

For small mixing angle (θ_V), $\cos 2\theta_V \sim 1$, so the survival probability, $\tilde{P}$ (equation (2.36)) will be described by the Landau-Zener formula (see equation (2.37)) [12], with E_{na}:

$$E_{na} \approx \Delta m^2 l_n \sin^2 2\theta_V. \tag{3.15}$$

In this approximation, we can find the following analitic relation between neutrino parameters:

$$\sin^2 2\theta_V \approx \frac{E \ln \tilde{P}(E)}{\Delta m^2 l_n} \tag{3.16}$$

The weaking of suppression ($\tilde{P} \rightarrow 1$), for fixed Δm^2, correspond to a decrease of $\sin^2 2\theta_V$. From condition (i) at sect. 3.1, we can estimate that the survival probability ($\tilde{P}$) should be

$$0.3 \lesssim \tilde{P} \lesssim 0.5 \tag{3.17}$$

for $f_B = 1$. From this interval of $\tilde{P}$ and from the previous formula we can find a bound for $\sin^2 2\theta_V$ and Δm^2.

To do this, we need a value of the parameter l_n. By using the following approximation for the electron density, valid in the most region of the Sun [14]:

$$n_e(x) = n_e(0) e^{-\frac{x}{r_0}} \tag{3.18}$$

it is easy to find

$$l_n \equiv \left| \frac{d}{dx} \ln n_e \right|^{-1} = r_0 \tag{3.19}$$

and with a good approximation, r_0 is equal to $0.1 \quad R_\odot \quad (R_\odot = 6.96 \ \ 10^5 \ \ km)$. In formula (3.16), we choose the energy which correspond to the maximum of the products

$$\phi_B^{SSM} \sigma_H \rightarrow 10.0 \ \ MeV \ \ , \ \ \phi_B^{SSM} \sigma_K \rightarrow 10.5 \ \ MeV \tag{3.20}$$

which appear in effective suppression factors P_H, P_K (3.3). In this way, we can find the region which is shown in Figure (3.2). The overlapping of this region with the general bound of section 3.2 will give us the "allowed region" for neutrino parameters.

Consider now the case $f_B \neq 1$. According to the condition **ii)** from section 3.1, we can neglect Q_{Ar}^{oth} in the formula (3.6) for the ^{37}Ar production-rate . In this case, we can write:

$$R_{Ar} = f_B P_H k_B \tag{3.21}$$

where R_{Ar} is fixed by experiments. Thus

$$f_B \propto \frac{1}{P_H} \tag{3.22}$$

the smaller f_B weakes the suppression of Boron neutrino flux due to MSW effect. By using this and equation (3.13) we can find the following relation

$$\sin^2 2\theta_V = \sin^2 2\theta_V^{SSM} \left[1 - \frac{\ln f_B}{\ln \tilde{P}^{SSM}}\right] \tag{3.23}$$

where $\tilde{P}^{SSM} \approx 0.4$ correspond to the SSM description ($f_B = 1$). From the formula (3.23) we can see that if f_B decrease the allowed region shift to smaller $\sin^2 2\theta_V$. Also the contribution of ν_μ to Kamiokande experiment diminishes with f_B:

$$\triangle\, R_{\nu_e}(\nu_\mu) = f_B r \left(1 - \frac{R_{\nu_e}}{f_B}\right) \tag{3.24}$$

This is true if P_K is not too small and $f_B > R_{\nu_e}$. From the formula (3.24), we can deduce $\Delta R_{\nu_e}(\nu_\mu) \to 0$ if $f_B \to R_{\nu_e} \sim 0.41 \div 0.51$. In this limit the double ratio (3.8) will be

$$R_{H/K} \approx k_B \approx 0.775 \tag{3.25}$$

This number should be compared with experimental value (3.9). 0.4$\div$ 0.5. Moreover, Q_{Ar}^{oth} increase for small f_B and this increases the double ratio: $R_{H/K} \approx k_B + \frac{Q_{Ar}^{oth}}{Q_{Ar}^{SSM}}$. This makes worse the fit, and gives the lower bound on $f_B = 0.4 \div 0.5$.

The maximal value of f_B can be found in the following way. By using the Homestake signal (3.6), we can rewrite the Kamiokande signal as

$$R_{\nu_e} = r f_B + \frac{(1-r)}{k_B} \frac{P_K}{P_H} R_{Ar} \tag{3.26}$$

where we neglect the contributions from the "other fluxes". From this relation, we can estimate the maximum value of f_B. We will choose the minimum value of the ratio $\frac{P_K}{P_H} = 0.895$ from the Table 3.1. The maximum $f_B^{max} = 2.15$ correspond to 95% $C.L.$. Thus in the small mixing case, we have:

$$0.4 < f_B < 2.15 \tag{3.27}$$

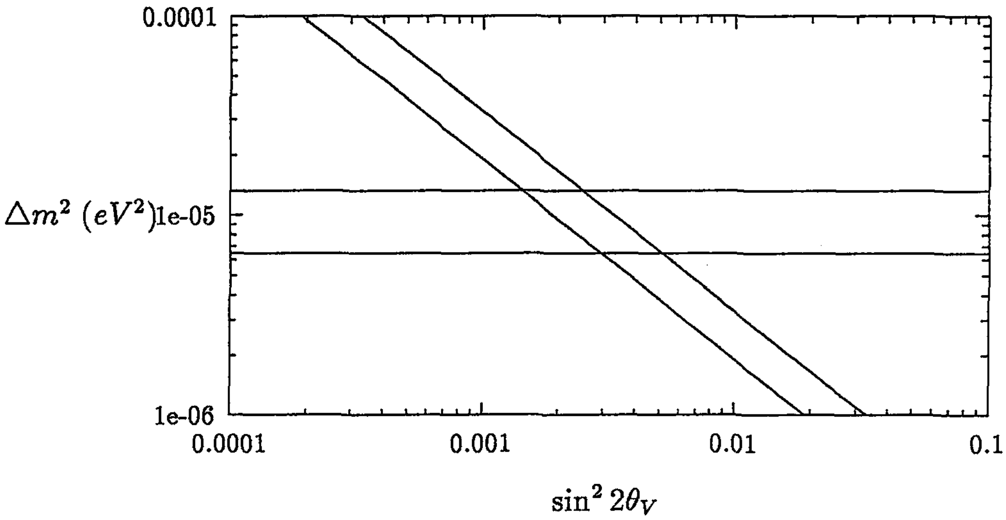

Figure 3.2: The allowed region for small mixing case (f_B=1).

In the Figure (4.1,4.2) are shown the alowed regions of parameters for $f_B = 1.5, 1.0, 0.75, 0.5$.

3.4 Large Mixing Solution

In the case of the large mixing solution, the high energy part of Boron neutrino flux is in the region in which the survival probability is independent on E. The survival probability has the asymtotic value corresponding to high energy limit of (2.32), and:

$$\tilde{P} \approx P_H \approx P_K \approx \sin^2\theta_V \tag{3.28}$$

In this approximation the Kamiokande signal becomes

$$R_{\nu_e} = f_B \left(\sin^2\theta_V + r(1 - \sin^2\theta_V)\right) \tag{3.29}$$

By using this formula and fixing $f_B = 1$, we can find the bound on $\sin^2 2\theta_V$ as

$$0.82 < \sin^2 2\theta_V < 0.99 \tag{3.30}$$

From Homestake signal we can write

$$Q_{Ar} = f_B P_H Q_{Ar}^{SSM} \tag{3.31}$$

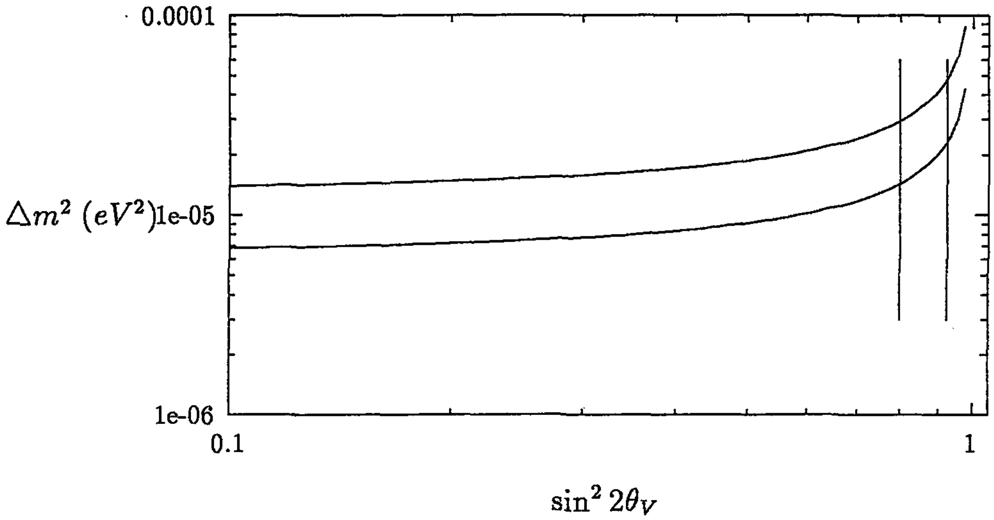

Figure 3.3: The allowed region for large mixing case (f_B=1).

which is right because the probability does not depend on energy. For $f_B = 1$, we can easily deduce the bound on $\sin^2 2\theta_V$ as

$$0.80 < \sin^2 2\theta_V < 0.92 \tag{3.32}$$

The upper in (3.32) is more strong than that in (3.30).

The maximal value of f_B is fixed by the increasing contribution to R_{ν_e} from ν_μ neutrinos. When f_B increases, the suppresion factor P_i decrease (see the equation (3.31)) and Q_{Ar}^{oth} diminishes. In the same time the contribution of the ν_μ to Kamiokande signal increase. From the experimental bound on the double ratio we can deduce the minimum for $\sin^2 \theta_V$=0.02 and $f_B^{max} \approx 3.4$.

Taking in account the region of the neutrino parameters which we found in the independent way in section 3.2, and using the bound for $\sin^2 2\theta_V$ in (3.32), we will find the allowed region for Δm^2 and $\sin^2 2\theta_V$.

From Figure (4.1,4.2) we can see that when f_B increases, the allowed region shifts to smaller mixing angles.

CHAPTER 4

CONCLUSION

The description of the existing data in terms of **MSW theory** gives the constraints on the neutrino parameters $\left(\Delta m^2,\, \sin^2\theta_V\right)$.

• In the **small mixing** case the allowed region for the parameters can be estimated by using simultaneously the condition (3.10) and the relation (3.16), which comes from the **Landau-Zener** formula. The present experimental data give the following bounds ($f_B = 1$):

$$\begin{aligned} \Delta m^2 &\sim 6.5\ 10^{-6} \div 1.3\ 10^{-5} \quad eV^2 \\ \sin^2\theta_V &\sim (1.4 \div 5.1)\ 10^{-3} \end{aligned}$$

• In the **large mixing** case we use the general condition (3.12) (from $E_{pp}^{max} < E_{res} < E_{Be}$) and the formulas (3.29,3.31) for the Kamiokande signal and the Homestake signal. We obtain from Homestake experiment for $f_B = 1$:

$$\begin{aligned} \Delta m^2 &\sim (1.45 \div 4.70)\ 10^{-5} \quad eV^2 \\ \sin^2\theta_V &\sim 0.80 \div 0.92 \end{aligned}$$

• With diminishing f_B the region of small mixing solutions is shifted to smaller $\sin^2 2\theta_V$. On the contrary the region of large mixing solution is shifted to small θ_V when f_B increases. (see Figure (4.1,4.2))

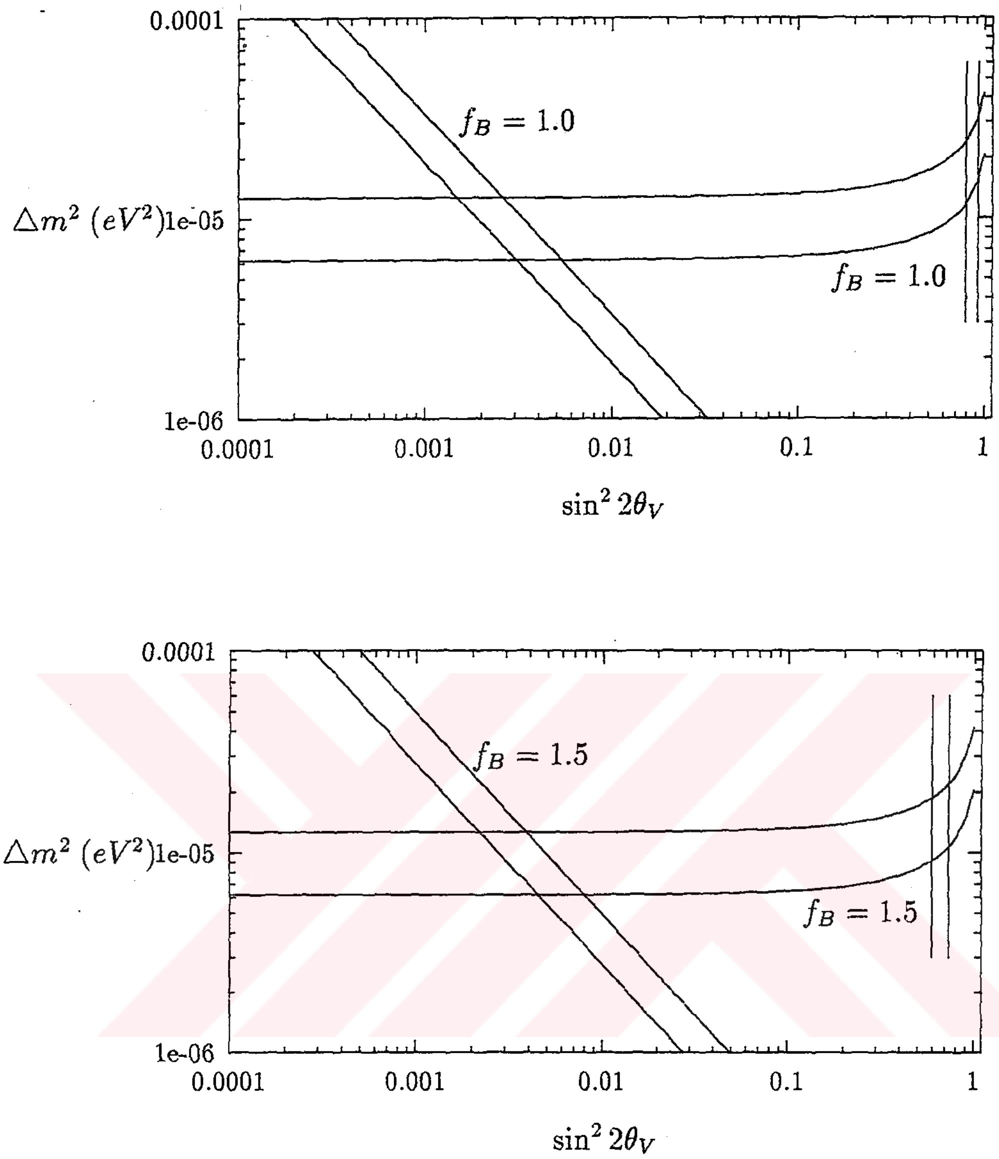

Figure 4.1: Allowed regions for large mixing case: $f_B = 1, 1.5$ and for small mixing solution: $f_B = 1, 1.5$ (PART I).

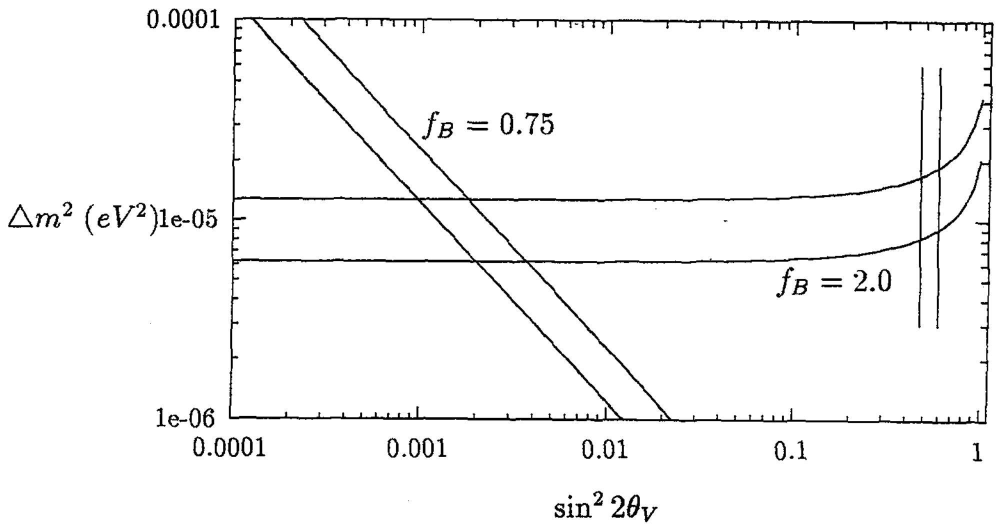

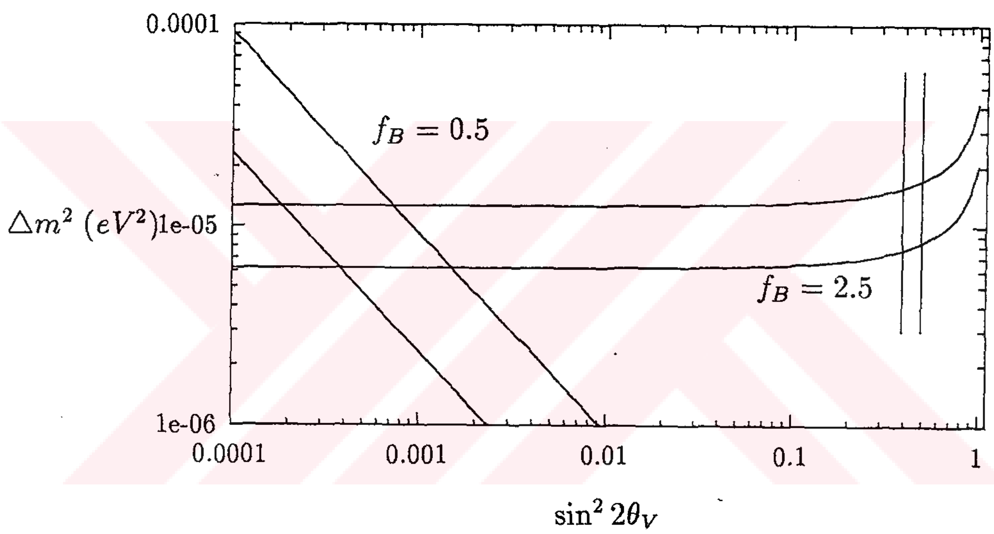

Figure 4.2: Allowed regions for large mixing case: $f_B = 2, 2.5$ and for small mixing solution: $f_B = 0.75, 0.5$ (PART II).

REFERENCES

[1] BAHCALL J. N. and ULRICH R. K. , Rev. Mod. Phys. 60, 297 (1985).

[2] BAHCALL J. N. and PINSONNEAULT M. M. , Rev. Mod. Phys. 64, 885 (1992).
HATA N. and LANGACKER P. , Preprint UPR-0592T.

[3] DAVIS R. Jr., Proc. of the 23^{th} ICRC, Calgary, Canada (1993), Prog. in Nucl. and Part. Phys. 32 (1994), LANDE K. talk given at "Neutrino-94".

[4] HIRATA K. S. et al, Phys. Rev. Lett. 66, 9 (1991); Phys. Rev. D44, 2241 (1991).
SUZUKI Y. , in TAUP-93.

[5] ABASOV A. I. et al, Phys. Rev. Lett. 67, 3332 (1991).
ABDURASHITOV J. N. et al, Phys. Lett. **B328**, 234 (1994).
GAVRIN V. N. , Talk given at Int Symposium " Nuetrino Telescopes", Venice,February, 377 (1994).

[6] ANSELMANN P. et al., Phys. Lett. **B285**, 376, 390 (1992); ibidem**B314**, 445 (1993); ibidem Phys. Lett. **B327**, 377 (1994).

[7] WOLFENSTEIN L., Phys. Rev. D **17**, 2369 (1978); Phys. Rev. D **20**, 2634 (1979).
MIKHEYEV S. P. and SMIRNOV A. Yu. , Sov. J. Nucl. Phys. 42, 913 (1985); Sov. Phys. JETP 64, 4 (1986); Nuovo Cimento **9C**, 17 (1986); Usp. Fiz. Nauk **153**,3 (1987).

[8] MIKHEYEV S. P. and SMIRNOV A. Yu., Prog. Part. Nucl. Phys. 23, 41 (1989).

[9] MIKHEYEV S. P. and SMIRNOV A. Yu. in "Neutrinos",Graduate text in-contempupary physics, edit by KLAPDOR H. V. (1988), p. 239.
MIKHEYEV S. P. and SMIRNOV A. Yu., Proceeding of the 12^{th} InternationalConference on Neutrino Physics and Astrophysics Sendai, June 3-8, 1986, p. 177.

[10] SMIRNOV A. Yu., Solar Neutrinos: Theoretical Aspects, Talk given atInst. Workshop on " Cosmological Dark Matter", Valencia-Spain, October 1993 to be published.

[11] HAXTON W. Phys. Rev. Lett. 57, 1271 (1986).
PARKE S. J., Phys. Rev. Lett. **57**, 1275 (1986); Conference of the 14^{th} SLAC Summer Institute on Particle Physics, Agust 5-8, 1986.

[12] LANDAU L. D., Phys. Z. USSR 1, 426 (1932).
ZENER C., Proc. R. Soc. A 137, 696 (1932).

[13] KRASTEV P. I. and SMIRNOV A. Yu., Report DOE/ER/40561-137-INT94-13-02.

[14] KRASTEV P. I. and PETCOV S. T., Phys. Lett. **B** 207, 64 (1989).

CURRICULUM VITAE

Hilmiye Balkan was born in İstanbul, 6 May, 1970. She graduated from Pertevniyal Lisesi in 1987 and from Physics Department of İstanbul University in 1991. She got schoolarship from Balkan Physics Union for Diploma Course Programme in ICTP. Then she got diploma from ICTP in 1994. She is a M.Sc. student of the physics program of İstanbul Technical University.